Original Article

MOLECULAR METABOLISM

Pnpla3 silencing with antisense oligonucleotides ameliorates nonalcoholic steatohepatitis and fibrosis in *Pnpla3* I148M knock-in mice

Daniel Lindén [1,2,], Andrea Ahnmark [1], Piero Pingitore [3], Ester Ciociola [3], Ingela Ahlstedt [1], Anne-Christine Andréasson [1], Kavitha Sasidharan [3], Katja Madeyski-Bengtson [4], Magdalena Zurek [5], Rosellina M. Mancina [3], Anna Lindblom [1], Mikael Bjursell [4], Gerhard Böttcher [5], Marcus Ståhlman [3], Mohammad Bohlooly-Y [4], William G. Haynes [1], Björn Carlsson [6], Mark Graham [7], Richard Lee [7], Sue Murray [7], Luca Valenti [8], Sanjay Bhanot [7], Peter Åkerblad [1], Stefano Romeo [3,9,10,*]**

ABSTRACT

Objective: Nonalcoholic fatty liver disease (NAFLD) is becoming a leading cause of advanced chronic liver disease. The progression of NAFLD, including nonalcoholic steatohepatitis (NASH), has a strong genetic component, and the most robust contributor is the patatin-like phospholipase domain-containing 3 (*PNPLA3*) rs738409 encoding the 148M protein sequence variant. We hypothesized that suppressing the expression of the PNPLA3 148M mutant protein would exert a beneficial effect on the entire spectrum of NAFLD.

Methods: We examined the effects of liver-targeted $GalNAc_3$-conjugated antisense oligonucleotide (ASO)-mediated silencing of *Pnpla3* in a knock-in mouse model in which we introduced the human *PNPLA3* I148M mutation.

Results: ASO-mediated silencing of *Pnpla3* reduced liver steatosis ($p = 0.038$) in homozygous *Pnpla3* 148M/M knock-in mutant mice but not in wild-type littermates fed a steatogenic high-sucrose diet. In mice fed a NASH-inducing diet, ASO-mediated silencing of *Pnpla3* reduced liver steatosis score and NAFLD activity score independent of the *Pnpla3* genotype, while reductions in liver inflammation score ($p = 0.018$) and fibrosis stage ($p = 0.031$) were observed only in the *Pnpla3* knock-in 148M/M mutant mice. These responses were accompanied by reduced liver levels of Mcp1 ($p = 0.026$) and Timp2 ($p = 0.007$) specifically in the mutant knock-in mice. This may reduce levels of chemokine attracting inflammatory cells and increase the collagenolytic activity during tissue regeneration.

Conclusion: This study provides the first evidence that a Pnpla3 ASO therapy can improve all features of NAFLD, including liver fibrosis, and suppress the expression of a strong innate genetic risk factor, *Pnpla3* 148M, which may open up a precision medicine approach in NASH.

Keywords PNPLA3; NAFLD; NASH; Fibrosis; Liver

1. INTRODUCTION

In parallel with the global increase in obesity, nonalcoholic fatty liver disease (NAFLD) is becoming the leading cause of chronic liver disease and liver transplantation worldwide [1]. NAFLD is defined as excess liver fat accumulation greater than 5% induced by causes other than alcohol intake. NAFLD progresses to liver inflammation (nonalcoholic steatohepatitis, NASH) and fibrosis in a variable proportion of individuals, ultimately leading to liver failure and hepatocellular carcinoma (HCC) in susceptible individuals [2]. The most important medical need in patients with NAFLD and NASH is an effective treatment to halt the progression and possibly reverse fibrosis, which is the main predictor of liver disease evolution [3,4].

Recently, we reported evidence suggesting that genetically determined hepatic fat accumulation is a major driver of NASH and fibrosis [5]. Indeed, the progression of NAFLD has a strong genetic component [6]. The rs738409 polymorphism in the patatin-like phospholipase domain-containing 3 (*PNPLA3*) gene (resulting in a change

[1]Cardiovascular, Renal and Metabolism, IMED Biotech Unit, AstraZeneca, Gothenburg, Sweden [2]Division of Endocrinology, Department of Neuroscience and Physiology, Sahlgrenska Academy, University of Gothenburg, Sweden [3]Department of Molecular and Clinical Medicine, University of Gothenburg, Sweden [4]Translational Genomics, Discovery Sciences, IMED Biotech Unit, AstraZeneca, Gothenburg, Sweden [5]Drug Safety & Metabolism, IMED Biotech Unit, AstraZeneca, Gothenburg, Sweden [6]Cardiovascular, Renal and Metabolism Translational Medicine Unit, Early Clinical Development, IMED Biotech Unit, AstraZeneca, Gothenburg, Sweden [7]Ionis Pharmaceuticals, Carlsbad, USA [8]Internal Medicine and Metabolic Diseases, Fondazione IRCCS Ca' Granda Ospedale Maggiore Policlinico Milano, Department of Pathophysiology and Transplantation, Università degli Studi di Milano, Milan, Italy [9]Clinical Nutrition Unit, Department of Medical and Surgical Sciences, Magna Graecia University, Catanzaro, Italy [10]Cardiology Department, Sahlgrenska University Hospital, Gothenburg, Sweden

*Corresponding author. Wallenberg Laboratory, Bruna Stråket 16, Department of Molecular and Clinical Medicine, University of Gothenburg, SE-413 45 Göteborg, Sweden. E-mail: stefano.romeo@wlab.gu.se (S. Romeo).

**Corresponding author. Cardiovascular, Renal and Metabolism, IMED Biotech Unit, AstraZeneca Gothenburg, SE-431 83 Mölndal, Sweden. E-mail: daniel.linden@astrazeneca.com (D. Lindén).

Received December 8, 2018 • Revision received January 22, 2019 • Accepted January 30, 2019 • Available online 5 February 2019

https://doi.org/10.1016/j.molmet.2019.01.013

List of abbreviations

ALT	alanine aminotransferase
ASK1	apoptosis signal-regulating kinase 1
αSma	alpha-smooth muscle actin
ASO	antisense oligonucleotide
AST	aspartate aminotransferase
AU	arbitrary unit
cEt	constrained ethyl
Col1a1	collagen type I alpha 1 chain
Ctrl	control
CVC	cenicriviroc
FBS	fetal bovine serum
FXR	farnesoid X receptor
$GalNAc_3$	triantennary N-acetylgalactosamine
GLP1	glucagon-like peptide-1
I	isoleucine
Il	interleukin
HCC	hepatocellular carcinoma
H&E	hematoxylin-eosin
HSD17B13	hydroxysteroid 17-beta dehydrogenase 13
Mac2	macrophage antigen 2
Mcp1	monocyte chemoattractant protein 1
MEM	minimum essential medium
Mmp2	matrix metalloproteinase 2
MOE	methoxyethylribose
MRI	magnetic resonance imaging
MUFA	monounsaturated fatty acid
NAFLD	nonalcoholic fatty liver disease
M	methionine
MUT	mutant
NAS	NAFLD activity score
NASH	nonalcoholic steatohepatitis
OCA	obeticholic acid
ORO	Oil Red O
PDFF	proton-density fat fraction
Plin2	perilipin 2
PNPLA3/Pnpla3	human/mouse patatin-like phospholipase domain-containing 3
PUFA	polyunsaturated fatty acid
Rplp0	ribosomal protein large P0
siRNA	small interfering RNA
SFA	saturated fatty acid
Tgfβr2	transforming growth factor, beta receptor 2
Timp	tissue inhibitor of metalloproteinase
Tnfα	tumor necrosis factor alpha
WT	wild-type

from isoleucine (I) to methionine (M) at position 148 of the protein) exerts the largest effect on NAFLD progression identified to date [7,8]. Furthermore, excess body fat amplifies the genetic risk of *PNPLA3* 148M on NAFLD [9–11]. The PNPLA3 protein has hydrolase activity towards triglycerides and retinyl esters [12–15], promoting lipid droplet remodeling in hepatocytes and hepatic stellate cells [16,17]. The PNPLA3 148M mutant protein exhibits reduced enzymatic activity [12–17].

Pnpla3 148M mutant knock-in mice develop hepatic steatosis when fed a steatogenic high-sucrose diet [18]. Similarly, mice overexpressing the human 148M mutant form of PNPLA3 exhibit elevated hepatic steatosis when fed a high-sucrose diet [19], whereas genetic *Pnpla3* deletion from birth does not influence hepatic fat accumulation in mice [20,21]. The mechanism underlying the *Pnpla3* 148M mutation—mediated increase in hepatic steatosis does not seem to involve increased lipogenesis or decreased fatty acid oxidation [15], but it is partially due to very low-density lipoprotein retention, at least in very obese individuals [15,16,22]. Moreover, the *Pnpla3* 148M mutation alters the posttranslational modification of Pnpla3. Wild-type Pnpla3 is catabolized through proteasomal degradation via effective ubiquitylation, whereas the Pnpla3 148M mutant protein escapes ubiquitylation and subsequently accumulates on the surface of lipid droplets, leading to impaired mobilization of triglycerides from the hepatic lipid droplets [15]. Based on the results of these preclinical studies, reduced expression of the PNPLA3 148M mutant protein may exert beneficial effects on NAFLD and potentially on NASH and liver fibrosis progression. This hypothesis is also supported by human genetic data. Indeed, we have shown that another *PNPLA3* genetic variant (rs2294918), which is associated with lower hepatic PNPLA3 expression, mitigates the detrimental impact of the PNPLA3 148M mutant protein [23]. Consistent with these data, a sequence variant in the hydroxysteroid 17-beta dehydrogenase 13 (*HSD17B13*) gene was recently shown to be associated with lower PNPLA3 expression and reduced the detrimental impact of the PNPLA3 148M protein [24]. Interestingly, the suppression of wild-type Pnpla3 expression with an antisense oligonucleotide (ASO) reduced the liver fat contents in rats fed a high-fat diet by diminishing fatty acid esterification [25]. This finding is consistent with data reported by Kumari et al. showing that Pnpla3 also promotes lipogenesis [26].

Taken together, we hypothesized that the suppressed expression of the PNPLA3 148M mutant protein would exert a beneficial effect on the entire spectrum of NAFLD including fibrosis. In this study, we tested this hypothesis by silencing Pnpla3 *in vivo* using a liver-targeted ASO treatment in *Pnpla3* I148M knock-in mice fed steatogenic and NASH-inducing diets.

2. MATERIALS AND METHODS

2.1. Screening and selection of murine *Pnpla3* cEt 5′-$GalNAc_3$-conjugated cEt ASOs

S-constrained ethyl (cEt)-modified 16-mer ASOs targeting the mouse *Pnpla3* gene were screened and tested for potency in primary mouse embryonic cortical neurons via free uptake (data not shown). An optimal potent mouse (5′-TATTTTTGGTGTATCC-3′) cEt ASO lead was selected for all subsequent pharmacological studies. This mouse Pnpla3 ASO was modified by 5′-conjugation with triantennary N-acetylgalactosamine ($GalNAc_3$) to further enhance the liver cell targeting *in vivo* following subcutaneous administration [27]. The specificity of target knockdown was demonstrated using a chemistry-matched scrambled control $GalNAc_3$- conjugated ASO (5′-GGCCAA-TACGCCGTCA-3′). The control $GalNAc_3$-conjugated ASO did not affect body weight-gain, liver weight, plasma alanine aminotransferase (ALT) or liver triglyceride content when dosed at 10 mg/kg/week for six weeks in mice fed a NASH-inducing diet (D09100301, Research Diets, New Brunswick, NJ) as compared to saline vehicle controls (Supporting Figure 1).

2.2. Animals

All animal experiments were performed with humane care and were approved by the Gothenburg Ethics Committee for Experimental

Animals in Sweden. The holding facility has received full accreditation from the Association for Assessment and Accreditation of Laboratory Animal Care (AAALAC).

The human *PNPLA3* I148M mutation was introduced into the mouse *Pnpla3* gene by replacing the isoleucine codon with a methionine codon in amino acid position 148 of the mouse *Pnpla3* gene using homologous recombination (Supporting Figure 2A and B) as described in the Supporting Materials and Methods. Founders were backcrossed with C57BL/6N females to generate heterozygous *Pnpla3* 148I/M mice. Sequence-verified heterozygous *Pnpla3* 148I/M mice (Supporting Figure 2C) were intercrossed to generate experimental homozygous *Pnpla3* 148M/M and wild-type littermates (*Pnpla3* 148I/I) as control mice for the dietary challenge and ASO pharmacology studies. All experimental animals were verified to have the correct genotype using PCR before the study began and verified again using PCR after termination, as described in the Supporting Materials and Methods. A few experimental animals were also verified by cDNA sequencing (Supporting Figure 2D), as outlined in the Supporting Materials and Methods. All animals were housed in transparent Makrolon cages with aspen wood chip bedding and nesting material, and the temperature- (21 ± 1 °C) and humidity (50 ± 10%) of the holding facility were controlled. The mice had free access to tap water and food and were on a 12-h day/night cycle.

Female *Pnpla3* 148M/M ($n = 21$) and wild-type littermates ($n = 19$) (6–8 weeks of age) were fed a high-sucrose diet (70% sucrose diet; TD98090, Envigo, Huntingdon, UK) for 15 weeks. Female mice were used in this experiment to replicate the established model by Smagris et al. [18], who used female animals in their high-sucrose diet experiments. In addition, in a pilot experiment, female mice accumulated more triglycerides in the liver compared to male mice when fed this diet (Supporting Figure 3A). In addition, female mice fed the high-sucrose diet accumulated more liver triglycerides compared to mice fed a regular chow diet containing (energy percentage) 12% fat, 62% carbohydrates, and 26% protein, with a total energy content of 3 kcal/g (R3; Lactamin, Kimstad, Sweden) (Supporting Figure 3B). After 5 weeks of feeding on the high-sucrose diet, liver lipid levels were assessed using a magnetic resonance imaging (MRI)–derived marker, proton-density fat fraction (PDFF), as described in the Supporting Materials and Methods. The mice were then assigned to $GalNAc_3$-conjugated ASO study groups ($n = 9$–12 animals/group) based on randomized stratification for body weight and liver lipid contents before the treatment was initiated. During the last 8 weeks of the study, groups of mice were dosed with either the control ASO or Pnpla3 ASO (5 mg/kg/week administered by two subcutaneous injections per week with saline as vehicle). After 6 weeks of ASO dosing, liver lipid levels were again assessed using MRI. Before unfasted mice were euthanized at 8:00–10:00 AM, the mice were metabolically synchronized for 24 h by withdrawing the food from 8:00 AM to 8:00 PM and then allowed free access to the food again from 8:00 PM to 8:00 AM. Mice were euthanized with isoflurane (Forene, Abbot Scandinavia AB, Sweden), blood was collected and plasma isolated, livers were collected, and pieces (same position in the left lateral lobe for all mice) were fixed with 4% formaldehyde in PBS for histology or snap-frozen in liquid N_2 and stored at −80 °C.

Male *Pnpla3*148 M/M mice ($n = 17$) and wild-type littermates ($n = 17$) (6–8 weeks of age) were fed a diet high in fat (40%, containing 18% trans-fat), carbohydrates (40%, containing 20% fructose) and cholesterol (2%) (NASH diet; D09100301, Research Diets, New Brunswick, NJ) [28–30] for 26 weeks. In a separate experiment, liver *Pnpla3* mRNA, triglyceride content as well as plasma ALT levels were found to be elevated in wild-type male mice fed the NASH-inducing diet as compared to mice fed a regular chow diet (Supporting Figure 4). The mice were assigned to $GalNAc_3$-conjugated ASO study groups ($n = 8$–9 mice/group) based on body weight, and during the last 14 weeks, the mice were dosed with either the control ASO or Pnpla3 ASO (5 mg/kg/week administered by two subcutaneous injections per week with saline as vehicle). Before unfasted mice were euthanized at 8:00–10:00 AM, the mice were metabolically synchronized for 24 h as described above. Mice were euthanized with isoflurane (Forene, Abbot Scandinavia AB, Sweden), blood was collected and plasma isolated, livers were collected, and pieces (same position in the left lateral lobe for all mice) were fixed with 4% formaldehyde in PBS for histology or snap-frozen in liquid N_2 and stored at −80 °C.

2.3. Liver and plasma biochemistry

Non-anesthetized plasma glucose levels were measured in tail vein blood using a portable glucometer (Accu-Chek mobile®). Plasma insulin levels were measured using a mouse/rat Insulin kit from Meso Scale Discovery (K152BZC-1, Rockville Maryland USA). Liver triglyceride and plasma triglyceride, ALT, aspartate aminotransferase (AST) and haptoglobin levels were analyzed using an ABX Pentra 400 instrument (Horiba Medical, Irvine, California, USA), and liver hydroxyproline levels were measured with an ELISA, as outlined in the Supporting Materials and Methods.

2.4. Liver histology

Liver lipid Oil Red O and immunohistochemical staining (Mac-2 and Col1A1) of mouse liver sections are detailed in Supporting Materials and Methods. Fibrosis and components of the NAFLD activity score (NAS) were determined on terminal samples according to the methods reported by Kleiner et al. [31]. All histological assessments were performed by a pathologist who was blinded to the treatment.

2.5. RNA preparation and qPCR

Total RNA was isolated from cells using an RNeasy Mini Kit (Qiagen). First-strand complementary DNA and real-time quantitative PCR analyses were performed according to standard techniques, as outlined in the Supporting Materials and Methods.

2.6. Hepatic lipid droplet isolation

Lipid droplets were purified from frozen livers by sucrose density gradient ultracentrifugation as previously described [18] and as described in Supporting Materials and Methods.

2.7. Immunoblot analyses

The membranes were incubated with commercial antibodies (Supporting Table 1) except for the anti-Pnpla3 primary antibody (1:500), which was kindly provided by the Helen Hobbs laboratory at the University of Texas Southwestern Medical Center at Dallas, TX, USA.

2.8. Lipidomic analysis on lipid droplets

Lipidomic analyses was carried out by mass spectrometry as described in Supporting Materials and Methods.

2.9. Statistical analysis

Differences between groups were examined using 2-sided *t*-tests (GraphPad Prism v. 7.04, GraphPad Software, CA). Data were log-transformed before statistical analyses when appropriate (when data were skewed). A p value less than 0.05 was considered significant. Data are presented as the means ± standard errors of the means

(SEMs). Correction for multiple testing was applied for lipidomic analyses. Differences between categorical variables deriving from liver histology (Figure 3) were analyzed by binary logistic analyses.

3. RESULTS

3.1. *Pnpla3* silencing specifically reduces liver steatosis in *Pnpla3* mutant knock-in mice fed a high-sucrose diet

To drive hepatic lipogenesis and to evaluate the impact of *Pnpla3* silencing on hepatic fat accumulation, homozygous *Pnpla3* 148M/M (mutant) knock-in female mice and wild-type littermates were fed a high-sucrose diet (70%) for 15 weeks. During the last 8 weeks of the experiment, mice of the two genotypes were treated with $GalNAc_3$-conjugated Pnpla3 or $GalNAc_3$-conjugated control ASOs. No differences in body weight gain, food intake (Figure 1A and B, Supporting Figure 5A and B) or in ovarian white adipose tissue weight (Supporting Figure 6A) were observed between the groups. In addition, the Pnpla3 ASO treatment did not affect plasma glucose or insulin levels (Supporting Figure 7A and B). Compared to the control ASO, the Pnpla3 ASO treatment markedly reduced the hepatic expression of *Pnpla3* mRNA (98% reduction, $p < 0.0001$) and levels of Pnpla3 protein on lipid droplets in both *Pnpla3* mutant knock-in and wild-type mice (Figure 1C and D). The Pnpla3 ASO treatment did not affect the white adipose tissue expression of *Pnpla3* mRNA levels (Supporting Figure 8A).

Six weeks of the Pnpla3 ASO treatment reduced liver lipid levels by 20% in *Pnpla3* mutant knock-in mice, as measured by MRI (Figure 1F, $p = 0.025$, Supporting Figure 9). After 8 weeks of treatment, the *Pnpla3* mutant knock-in mice treated with the Pnpla3 ASO showed reduced liver weights (Supporting Figure 10A), lower liver Oil Red O staining of neutral lipids (Figure 1E), a 20% reduction ($p = 0.038$) in liver triglyceride content, as measured by biochemical analyses (Figure 1F), while no changes in circulating plasma triglyceride levels were observed (Figure 1G). Interestingly, the Pnpla3 ASO treatment did not affect the liver weights (Supporting Figure 10B), lipid level or liver triglyceride content in the wild-type mice (Figure 1H–J, Supporting Figure 9). *Pnpla3* mutant knock-in mice treated with the control ASO had 30% higher liver triglyceride content than the wild-type mice treated with the control ASO (*Pnpla3*mutant knock-in mice = 5.7 ± 0.4 g/100 g liver, wild-type mice = 4.4 ± 0.5 g/100 g liver, $p = 0.046$).

Thus, in a high-sucrose diet model of moderate hepatic steatosis, the Pnpla3 ASO treatment reduces the liver fat content in *Pnpla3* mutant knock-in mice but not in wild-type littermates.

3.2. *Pnpla3* silencing reduces liver inflammation and fibrosis specifically in the *Pnpla3* mutant knock-in mice fed a NASH-inducing diet

Next, we tested the hypothesis that *Pnpla3* silencing would reduce not only the liver fat content but also liver inflammation and fibrosis in a mouse model of diet-induced NASH. Male *Pnpla3* mutant knock-in ($n = 17$) and wild-type littermate ($n = 17$) mice were fed a NASH-inducing diet for 26 weeks. During the last 14 weeks of the experiment, mice of both genotypes were treated with a $GalNAc_3$-conjugated Pnpla3 or $GalNAc_3$-conjugated control ASO. No differences in body weight gain, food intake (Figure 2A and B, Supporting Figure 5C and D), or in epididymal white adipose tissue weight (Supporting Figure 6B) were observed between the groups. In addition, the Pnpla3 ASO treatment did not affect plasma glucose or insulin levels (Supporting Figure 7C and D). Compared to the control ASO, the Pnpla3 ASO treatment markedly reduced (97%, $p < 0.0001$) hepatic expression of the *Pnpla3* mRNA and consistently reduced levels of the Pnpla3 protein on lipid droplets in both *Pnpla3* mutant knock-in and wild-type mice (Figure 2C and D). Using the NASH diet with a longer treatment period than in the sucrose diet study (14 weeks *vs* 8 weeks, respectively), the Pnpla3 ASO treatment also reduced the white adipose tissue expression of *Pnpla3* mRNA levels (Supporting Figure 8B). The Pnpla3 ASO treatment reduced plasma ALT levels in mice of both genotypes (*Pnpla3* mutant knock-in $p = 0.0006$, wild-type $p = 0.018$), while plasma AST was unchanged (Figure 2E and F). The Pnpla3 ASO treatment reduced liver weights only in the *Pnpla3* mutant knock-in mice (Supporting Figure 10C–D), triglyceride contents in both *Pnpla3* mutant knock-in ($p = 0.002$) and wild-type mice ($p = 0.004$), while no changes in circulating plasma triglyceride levels were observed (Figure 2E and F). Thus, in severe steatosis, silencing of Pnpla3 expression in the liver reduces severe steatosis, regardless of the genetic background.

Overall, the genotype had no significant effect on liver damage assessed by histology. However, the Pnpla3 ASO treatment improved the liver steatosis score ($p = 0.007$), lobular inflammation score ($p = 0.018$), NAFLD activity score (NAS) ($p = 0.0003$), and fibrosis stage ($p = 0.031$) in *Pnpla3* mutant knock-in mice (Figure 3A) while only liver steatosis score ($p = 0.003$) and NAS ($p = 0.036$) were improved in the wild-type mice (Figure 3B). Hepatocellular ballooning degeneration was not found in any of the livers. This is an expected caveat with preclinical rodent NASH models in relation to human NASH and in line with another study using the same NASH diet feeding length in mice [30].

3.3. *Pnpla3* silencing reduces *de novo lipogenesis* and palmitoleic acid in *Pnpla3* mutant knock-in and wild-type mice fed a NASH-inducing diet

The Pnpla3 ASO treatment reduced the liver Oil Red O staining of neutral lipids in both *Pnpla3* mutant knock-in and wild-type mice (Figure 4A). The Pnpla3 ASO treatment reduced the mRNA expression of lipogenic genes, such as *acetyl-CoA carboxylase 1* (*Acc1*) and *stearoyl-CoA desaturase 1* (*Scd1*) in both genotypes (Figure 4B and C), suggesting that hepatic lipogenesis was reduced. Next, we examined the lipid composition of purified lipid droplets from the liver. Pnpla3 ASO treatment decreased the relative amount of monounsaturated fatty acids (MUFAs, $p = 6.1 \times 10^{-5}$ and 7.6×10^{-6} in the mutant and wild-type, respectively) and increased polyunsaturated fatty acids (PUFAs, $p = 1.2 \times 10^{-4}$ and 1.3×10^{-5} in the mutant and wild-type, respectively) irrespective of the genotype (Figure 4D and E, Table 1, Supporting Table 2). Specifically, the reduction in MUFAs was stronger for the palmitoleic acid (16:1), 36% ($p = 2.4 \times 10^{-4}$) and 30% (1.0×10^{-9}) reduction for the mutant and wild-type, respectively as compared with the oleic acid where the reduction was only 2% ($p = 0.034$) and 5% ($p = 0.001$) for the mutant and wild-type, respectively.

3.4. *Pnpla3* silencing reduces protein levels of haptoglobin, Mcp1 and Timp2 specifically in the *Pnpla3* mutant knock-in mice fed a NASH-inducing diet

The Pnpla3 ASO treatment reduced plasma haptoglobin levels ($p = 0.0005$) and the liver macrophage content ($p = 0.047$) in *Pnpla3* mutant knock-in mice but not in the wild-type littermates (Figure 5A–C), suggesting that Pnpla3 suppression specifically reduced liver inflammation in the mutant mice. Pnpla3 ASO treatment specifically reduced the liver Mcp1 (Figure 5D) protein levels in *Pnpla3* mutant knock-in mice but not in wild-type mice. Pnpla3 ASO treatment did not change the liver protein expression levels of Il1β (Figure 5E), Il6 (Figure 5F), Tnfα (Figure 5G), or αSma (Figure 5H) in either genotype.

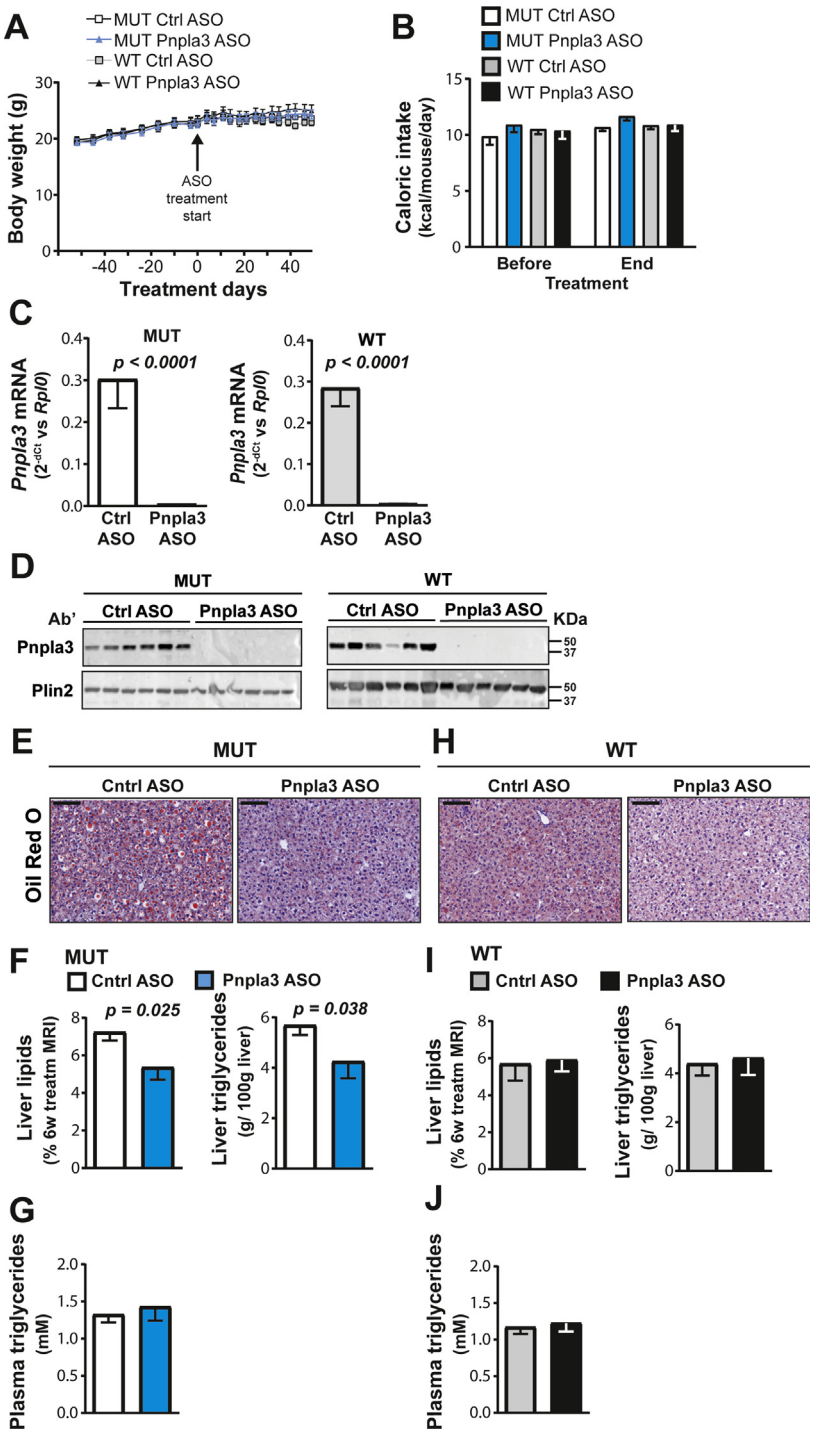

Figure 1: The Pnpla3 ASO treatment reduced liver *Pnpla3* mRNA and protein levels in both *Pnpla3* mutant knock-in mice and wild-type littermates fed a high-sucrose diet but reduced hepatic triglyceride content only in mutant mice. A total of 21 female homozygous *Pnpla3* 148M/M knock-in mice and 19 wild-type littermates were fed a high-sucrose diet for 15 weeks. After 7 weeks of feeding on the high-sucrose diet, mice were assigned to ASO study groups based on body weight and liver fat percentage, as assessed by MRI. *Pnpla3* mutant knock-in and wild-type mice were treated with either the control or Pnpla3 ASO (5 mg/kg/week administered by two subcutaneous injections per week, $n = 9–12$ mice/group) for 8 weeks. (A) Body weight gain before and after the ASO treatment. (B) Caloric intake before and after the ASO treatment. (C) Liver *Pnpla3* mRNA levels were measured by qPCR and normalized to the *ribosomal protein large P0* (*Rplp0*). (D) Levels of the Pnpla3 protein in hepatic lipid droplets were measured by western blotting. Plin2 was used as the loading control. Hepatic lipid droplets where purified by density gradient ultracentrifugation (see the Materials and Methods). (E,H) Representative images of Oil Red O-stained liver sections after 8 weeks of ASO treatment (black scale bar represents 100 μm). Liver lipid levels were assessed by MRI after 6 weeks of ASO treatment, and liver and plasma triglyceride levels were measured by biochemical assays when *Pnpla3* mutant knock-in (F–G) and wild-type (I–J) mice were euthanized after 8 weeks of ASO treatment. Values are presented as the mean ± SEM. *P* values were calculated using 2-sided *t*-tests. Abbreviations: ASO: antisense oligonucleotide; MRI: magnetic resonance imaging; Plin2: perilipin 2; Pnpla3: patatin-like phospholipase domain-containing 3; Rplp0: ribosomal protein large P0; AU: arbitrary unit; Ctrl: control. Mutant knock-in mice are defined as homozygotes for a methionine (M) at position 148 of the Pnpla3 protein, while wild-type littermates are homozygotes for an isoleucine (I) at the same position. WT: wild-type; MUT: mutant.

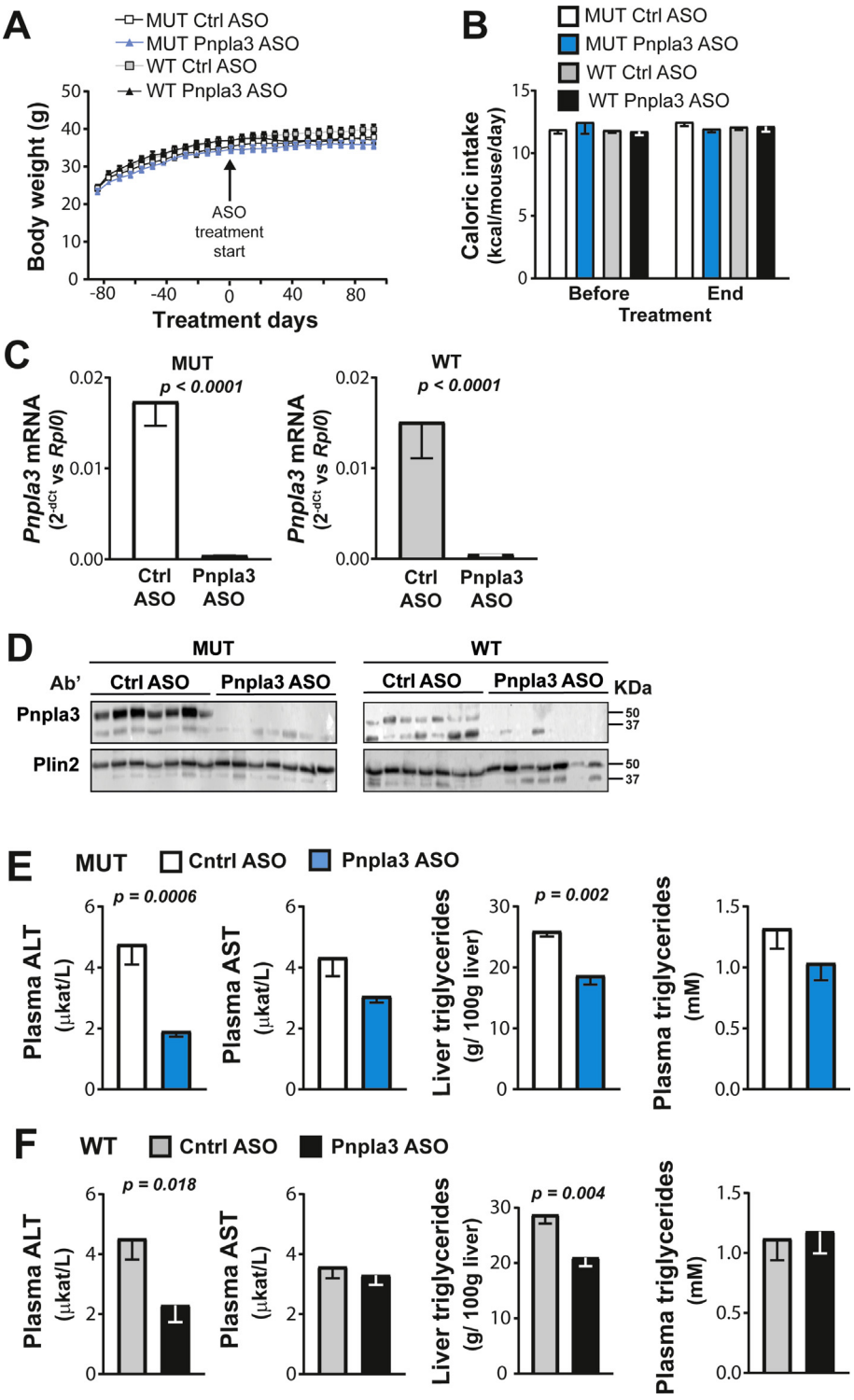

Figure 2: The Pnpla3 ASO treatment reduced liver *Pnpla3* mRNA and protein levels and liver triglyceride levels in both *Pnpla3* mutant knock-in mice and wild-type littermates fed a NASH-inducing diet. A total of 17 male homozygous *Pnpla3* 148M/M (mutant) knock-in mice and 17 wild-type littermates were fed a NASH-inducing diet for 26 weeks. After 12 weeks of consumption of the NASH diet, mice were assigned to ASO study groups based on body weight. *Pnpla3* mutant knock-in and wild-type mice were treated with either control or Pnpla3 ASOs (5 mg/kg/week administered by two subcutaneous injections per week, $n = 8–9$ mice/group) for 14 weeks. (A) Body weight was measured throughout the experiment, while (B) caloric intake was measured before and after the ASO treatment. (C) Liver *Pnpla3* mRNA levels were measured by qPCR and normalized to *Rplp0*. (D) Levels of the Pnpla3 protein in hepatic lipid droplets were measured by western blotting. Plin2 was used as the loading control. Hepatic lipid droplets were purified by density gradient ultracentrifugation (see the Materials and Methods). Plasma ALT, AST, and triglyceride levels and the liver triglyceride content in the *Pnpla3* mutant knock-in (F,G) and wild-type (I,J) mice were measured using biochemical assays. Values are presented as the mean ± SEM. *P* values were calculated using 2-sided *t*-tests. Abbreviations: ASO: antisense oligonucleotide; ALT: alanine aminotransferase; AST: aspartate aminotransferase; Plin2: perilipin 2; Pnpla3: patatin-like phospholipase domain-containing 3; Rplp0: ribosomal protein large P0; Ctrl: control; AU: arbitrary unit. Mutant knock-in mice are defined as homozygotes for a methionine (M) at position 148 of the Pnpla3 protein, while wild-type littermates are homozygotes for an isoleucine (I) at the same position. WT: wild-type; MUT: mutant.

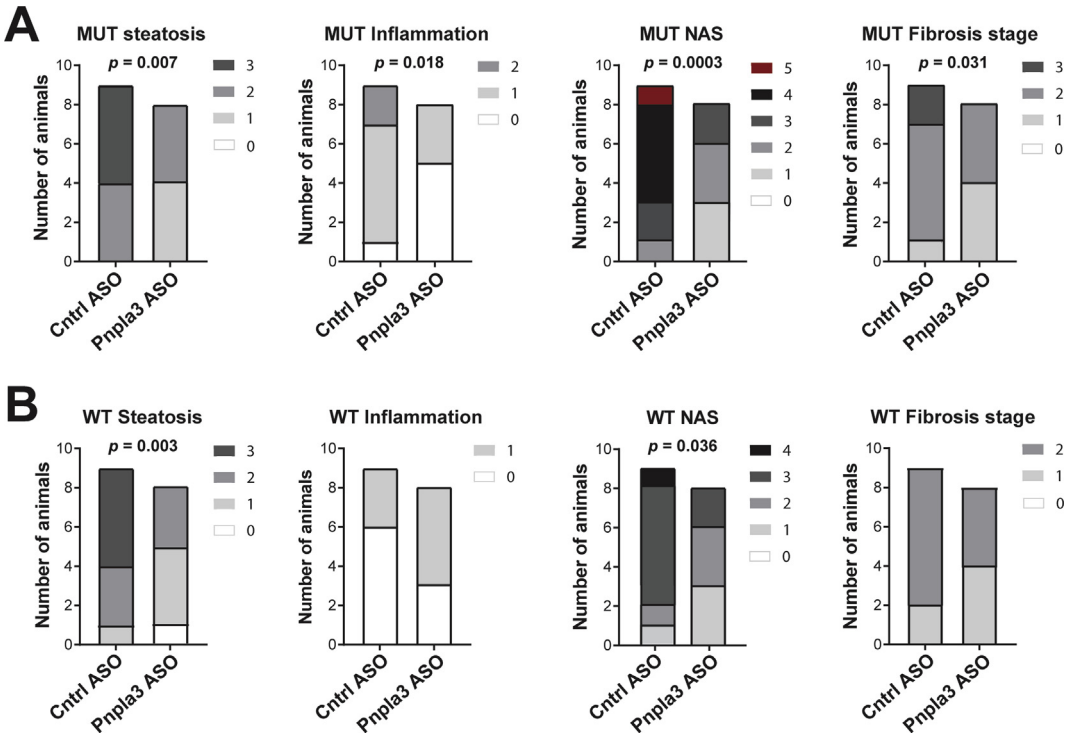

Figure 3: The Pnpla3 ASO treatment improved liver steatosis score, lobular inflammation score, NAFLD activity score, and fibrosis stage in *Pnpla3* mutant knock-in mice and steatosis score and NAFLD activity score in wild-type mice fed a NASH-inducing diet. Homozygous *Pnpla3* mutant knock-in and wild-type littermates were fed a NASH-inducing diet for 26 weeks. After 12 weeks of consuming the NASH diet, *Pnpla3* mutant knock-in and wild-type mice were treated with either control or Pnpla3 ASOs (5 mg/kg/week administered by two subcutaneous injections per week, $n = 8–9$ mice/group) for 14 weeks. Liver steatosis score, lobular inflammation score, NAS, and fibrosis stage in *Pnpla3* mutant knock-in (A) and wild-type (B) mice. *P* values were calculated using ordinal regression analyses. Abbreviations: NAS: NAFLD activity score: Pnpla3: patatin-like phospholipase domain-containing 3. Mutant knock-in mice are defined as homozygotes for a methionine (M) at position 148 of the Pnpla3 protein, while wild-type littermates are homozygotes for an isoleucine (I) at the same position. WT: wild-type; MUT: mutant.

The Pnpla3 ASO treatment reduced the hepatic expression of the *collagen type I alpha 1* (*Col1a1*) mRNA in both *Pnpla3* mutant knock-in and wild-type mice (Figure 6A and B). However, the Pnpla3 ASO treatment reduced the liver collagen, as measured by immunohistochemistry ($p = 0.04$), in only the *Pnpla3* mutant knock-in mice (Figure 6A–C). Although ASO treatment tended to decrease liver hydroxyproline levels, no significant differences were observed (Figure 6D and E). Interestingly, Pnpla3 ASO treatment specifically reduced the liver Timp2 protein levels in *Pnpla3* mutant knock-in mice ($p = 0.007$) but not in wild-type mice (Figure 7A). Pnpla3 ASO treatment did not change the liver protein expression levels of Mmp2 (Figure 7B), Timp1 (Figure 7C), or Tgfβr2 (Figure 7D) in either genotype. Thus, Pnpla3 suppression specifically reduced the liver collagen area and Timp2 protein levels in the *Pnpla3* mutant mice.

4. DISCUSSION

The major novel findings of this study are that *Pnpla3* silencing reduces liver inflammation and fibrosis in mutant mice homozygous for the *Pnpla3* 148M sequence variant demonstrating that a PNPLA3 ASO therapy can have beneficial effects on the entire spectrum of NAFLD. In our previous genetic association study in humans, the *PNPLA3* rs2294918 sequence variant, a variant associated with lower hepatic PNPLA3 expression, blunted the deleterious effect of the PNPLA3 148M mutant protein in subjects carrying this variant [23]. In addition, the *HSD17B13* rs72613567 sequence variant is associated with reduced *PNPLA3* mRNA expression and a decreased risk of liver injury in subjects carrying the PNPLA3 148M mutant protein [24]. Therefore, we hypothesized that suppression of the synthesis of this protein may be beneficial in homozygous carriers of the deleterious 148M protein. We generated knock-in mice homozygous for the *Pnpla3* mutant (148 M/M) protein by replacing the isoleucine codon with a methionine codon in amino acid position 148 of the mouse *Pnpla3* gene. First, we stimulated hepatic *de novo* lipogenesis by feeding mice a high-sucrose diet to assess the impact of *Pnpla3* silencing on moderate hepatic fat accumulation. To compare data with those previously reported by Smagris et al. [18], in this experiment, we used female mice and found, consistently with their study, that *Pnpla3* mutant knock-in mice had higher liver fat content than the wild-type littermates [18]. Pnpla3 suppression specifically resulted in a 25% reduction in hepatic steatosis in *Pnpla3* mutant knock-in mice, whereas hepatic fat accumulation was not affected by the treatment in wild-type littermates.

To investigate whether Pnpla3 silencing also ameliorated hepatic inflammation and fibrosis, we next fed male mice a NASH-inducing diet [28,29] (high fructose, fat and cholesterol). This diet-induced NASH model has already been proven useful to recapitulate the beneficial effects of compounds used in clinical trials for NASH on liver fat accumulation, inflammation and fibrosis [30]. The NASH diet resulted in an approximately 5-fold higher liver fat content (up to one-third of the total liver weight) as compared to the high-sucrose diet.

The lack of differences in liver fat content, inflammation, and fibrosis between *Pnpla3* mutant knock-in mice and wild-type mice on the NASH diet may due to; a) the very high amounts of calories and fat in the diet, which overrode the effect of the genotype, b) the more severe

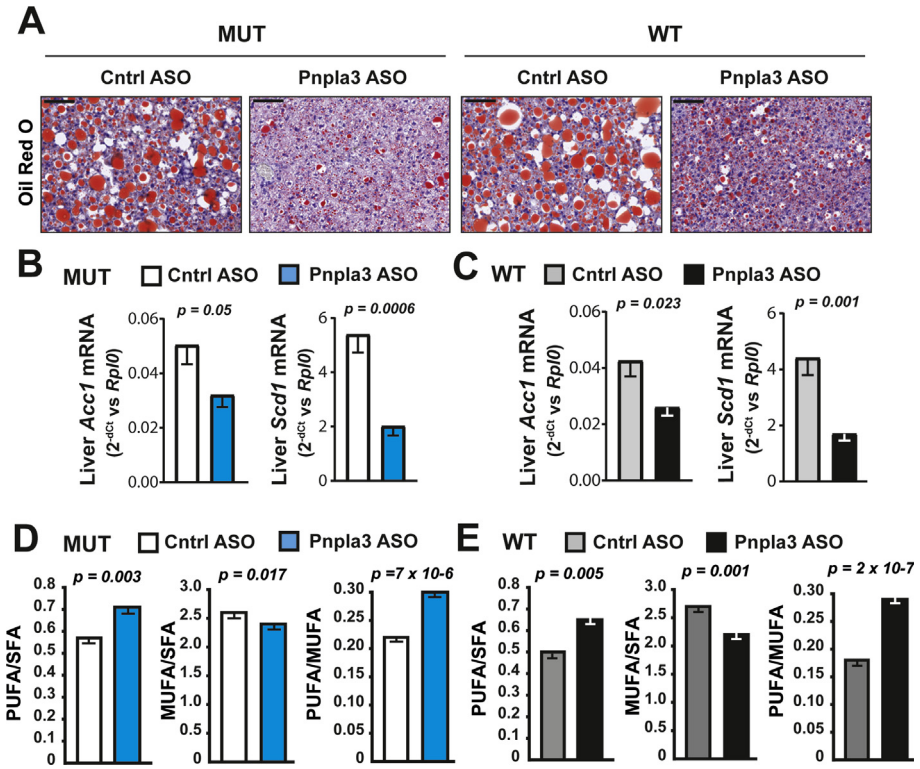

Figure 4: The Pnpla3 ASO treatment reduced liver steatosis, lipogenesis, and monounsaturated fatty acids in lipid droplets in *Pnpla3* mutant knock-in mice and wild-type littermates fed a NASH-inducing diet. Homozygous *Pnpla3* mutant knock-in and littermate wild-type mice were fed a NASH-inducing diet for 26 weeks. After 12 weeks of feeding on the NASH diet, *Pnpla3* mutant knock-in and wild-type mice were treated with either control or Pnpla3 ASOs (5 mg/kg/week administered by two subcutaneous injections per week, $n = 8–9$ mice/group) for 14 weeks. (A) Representative images of Oil Red O-stained liver sections (black scale bar represents 100 μm). Liver mRNA expression levels of *Acc1* and *Scd1* in *Pnpla3* mutant knock-in (B) and wild-type (C) mice. Liver lipid droplet fatty acid composition in *Pnpla3* mutant knock-in (D) and wild-type (E) mice. Values are presented as the mean ± SEM. *P* values were calculated using 2-sided *t*-tests. Abbreviations: Acc1: acetyl-CoA carboxylase 1; ASO: antisense oligonucleotide; Ctrl: control; MUFA: monounsaturated fatty acid; Pnpla3: patatin-like phospholipase domain-containing 3; PUFA: polyunsaturated fatty acid; Rplp0: ribosomal protein large P0; Scd1: stearoyl-CoA desaturase 1; SFA: saturated fatty acid. Mutant knock-in mice are defined as homozygotes for a methionine (M) at position 148 of the Pnpla3 protein, while wild-type littermates are homozygotes for an isoleucine (I) at the same position. WT: wild-type; MUT: mutant.

Table 1 — Composition of triglycerides in isolated hepatic lipid droplets from mutant knock-in (MUT) and wild-type (WT) mice measured by lipidomic analyses.

	MUT			WT		
	CTR	ASO	*P* value	CTR	ASO	*P* value
MUFA	63 (0.47)	58 (0.43)	6.1×10^{-5}	64 (0.39)	57 (0.58)	7.6×10^{-6}
16:1	10 (0.22)	7 (0.35)	2.4×10^{-4}	11 (0.17)	7 (0.13)	1.0×10^{-9}
18:1	53 (0.46)	52 (0.21)	0.034	54 (0.52)	51 (0.53)	0.001
PUFA	14 (0.29)	17 (0.50)	1.1×10^{-5}	12 (0.38)	17 (0.48)	1.3×10^{-6}
18:2	11 (0.42)	13 (0.48)	0.007	11 (0.35)	13 (0.49)	0.006
20:3	0.78 (0.03)	1.08 (0.05)	1.3×10^{-4}	0.53 (0.04)	1.01 (0.03)	3.3×10^{-5}
20:4	0.68 (0.02)	1.04 (0.03)	2.6×10^{-7}	0.31 (0.02)	1.09 (0.03)	1.2×10^{-7}
22:5	0.32 (0.05)	0.95 (0.05)	2.6×10^{-5}	0.07 (0.01)	0.90 (0.03)	9.1×10^{-9}
22:6	0.74 (0.17)	1.06 (0.09)	0.048	0.17 (0.01)	0.96 (0.03)	1.4×10^{-9}
SFA	24 (0.39)	25 (0.57)	0.999	24 (0.72)	26 (0.63)	0.141
14:0	0.47 (0.04)	0.41 (0.03)	0.275	0.46 (0.02)	0.40 (0.03)	0.122
16:0	22 (0.38)	22 (0.51)	0.693	22 (0.67)	24 (0.59)	0.093
18:0	1.3 (0.03)	1.8 (0.08)	4×10^{-4}	1.2 (0.06)	1.8 (0.06)	9×10^{-5}

Data are presented as mean (SEM). *P* values are calculated by *t* test and adjusted for multiple testing by Bonferroni. Individuals fatty acids are denoted as number of carbon and of double bonds.
Abbreviations: MUFA: Monounsaturated fatty acid; PUFA: Polyunsaturated fatty acid; SFA: Saturated fatty acid.

liver damage and fibrosis may have caused a progressive reduction of liver fat in the *Pnpla3* mutant knock-in mice, or c) a lack of statistical power to detect such differences. In addition, due to our study design, we cannot rule out an interaction between gender and diet in determining liver fat content.

In our study, *Pnpla3* silencing effectively reduced the liver fat and circulating ALT levels in both genotypes. This result is consistent with previous data obtained from wild-type rats fed a high-fat diet, where suppression of wild-type *Pnpla3* by an unconjugated 2′-O-methoxyethylribose (MOE) Pnpla3 ASO resulted in a reduction in the hepatic fat due to lower lipogenesis [25]. A likely explanation for the reduced liver steatosis in our model is also a reduced lipogenesis, as supported by lower expression of the *Acc1* and *Scd1* mRNAs.

To understand changes in the composition of fatty acids we purified hepatic lipid droplets from the mice and examined the triglyceride plethora by lipidomic analyses. Overall, the changes observed after ASO treatment were the same in the mutant as compared to the wild-type mice. Specifically, we observed lower levels of MUFAs in particular palmitoleic acid after Pnpla3 ASO treatment irrespective of the genotype. The lower abundance of palmitoleic acid is consistent with the lower levels of *Scd1*, the main enzyme responsible for desaturating fatty acids during lipogenesis. We found relatively higher

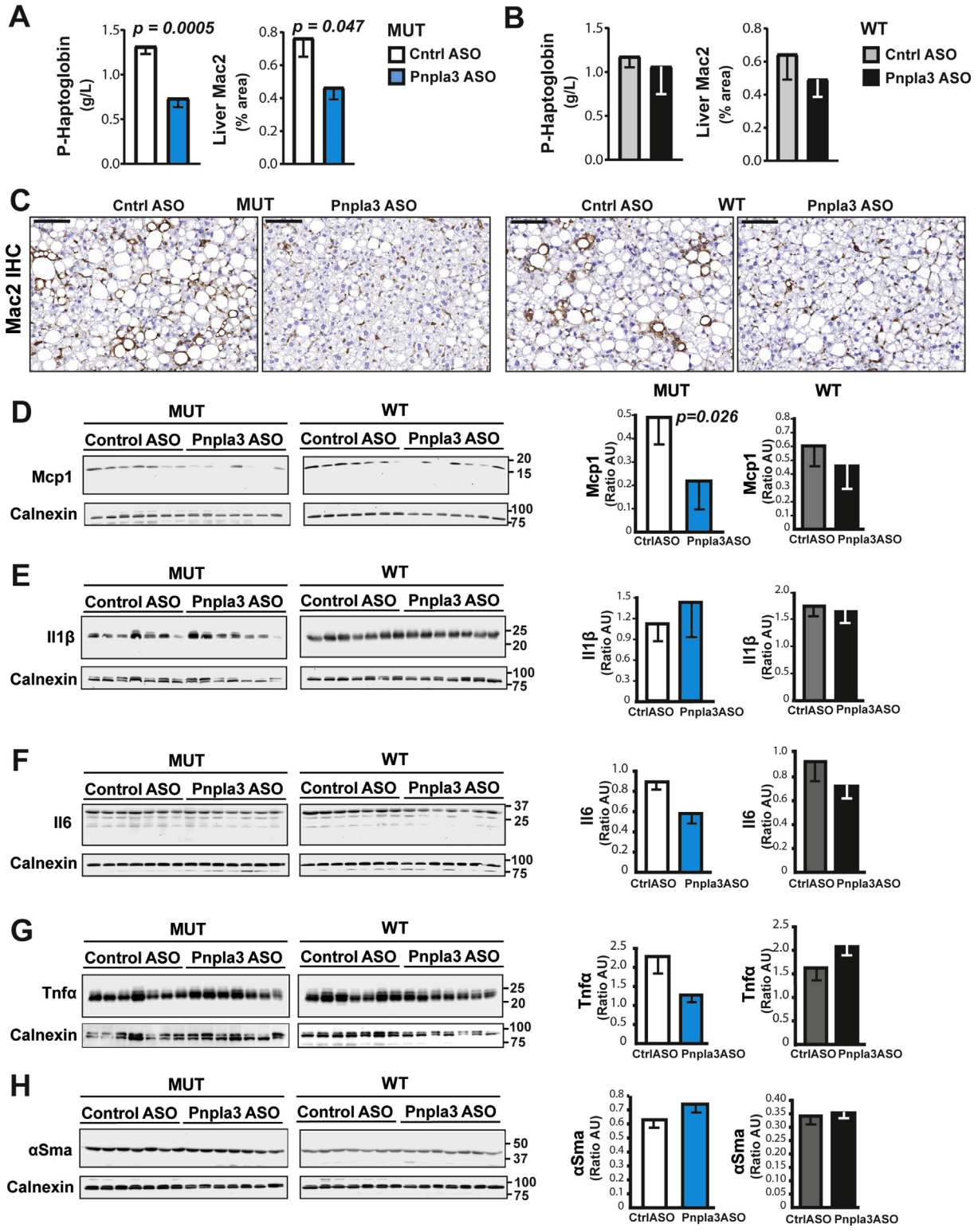

Figure 5: The Pnpla3 ASO treatment reduced plasma haptoglobin levels, liver macrophage content, and Mcp1 levels in *Pnpla3* mutant knock-in mice fed a NASH-inducing diet. Homozygous *Pnpla3* mutant knock-in and wild-type littermates were fed a NASH-inducing diet for 26 weeks. After 12 weeks of consuming the NASH diet, *Pnpla3* mutant knock-in and wild-type mice were treated with either control or Pnpla3 ASOs (5 mg/kg/week administered by two subcutaneous injections per week, $n = 8–9$ mice/group) for 14 weeks. Plasma haptoglobin levels and liver macrophage contents (as determined by Mac2 staining) in *Pnpla3* mutant knock-in (A) and wild-type (B) mice. (C) Representative images of Mac2-stained liver sections (black scale bar represents 100 μm). Liver protein levels of Mcp1 (D), Il1β (E), Il6 (F), Tnfα (G), and αSma (H) measured with western blot analyses. Values are presented as the mean ± SEM. *P* values were calculated using 2-sided *t*-tests. Abbreviations: αSma: alpha-smooth muscle actin; ASO: antisense oligonucleotide; Ctrl: control; Il: Interleukin; Mac2: macrophage antigen 2. Mcp1: monocyte chemoattractant protein 1; Pnpla3: patatin-like phospholipase domain-containing 3; Tnfα: tumor necrosis factor alpha. Mutant knock-in mice are defined as homozygotes for a methionine (M) at position 148 of the Pnpla3 protein, while wild-type littermates are homozygotes for an isoleucine (I) at the same position. WT: wild-type; MUT: mutant.

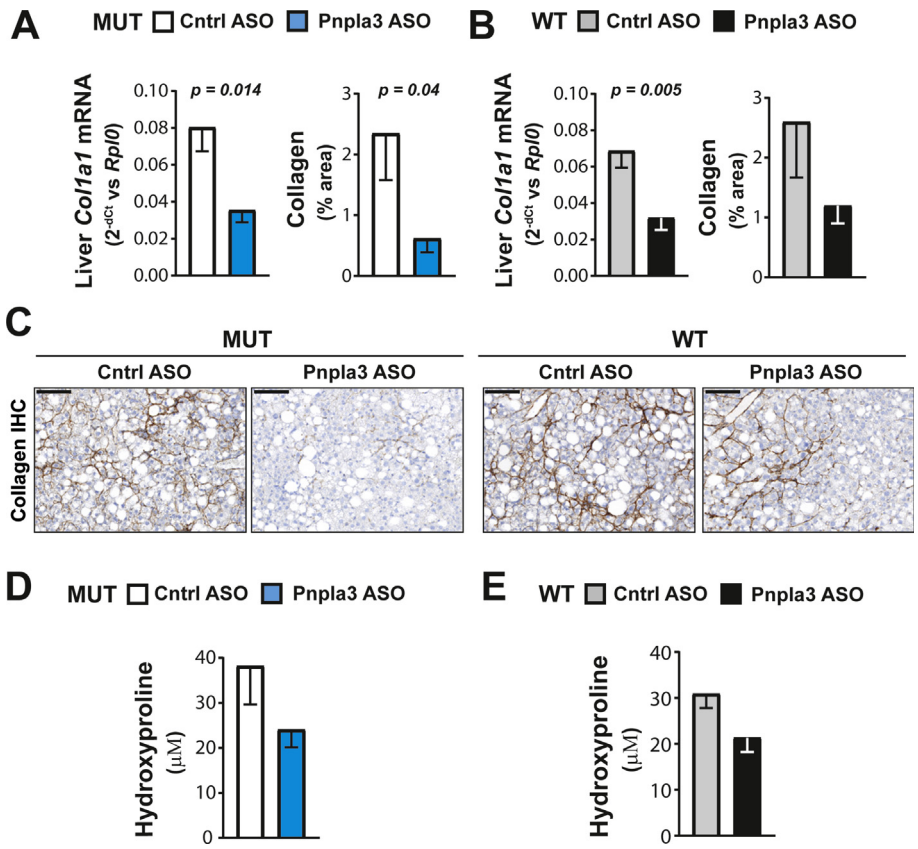

Figure 6: The Pnpla3 ASO treatment reduced liver fibrosis in *Pnpla3* mutant knock-in mice fed a NASH-inducing diet. Homozygous *Pnpla3* mutant knock-in and wild-type littermates were fed a NASH-inducing diet for 26 weeks. After 12 weeks of feeding on the NASH diet, *Pnpla3* mutant knock-in and wild-type mice were treated with either control or Pnpla3 ASOs (5 mg/kg/week administered by two subcutaneous injections per week, $n = 8–9$ mice/group) for 14 weeks. Liver *Col1a1* mRNA and protein (immunohistochemistry) levels in *Pnpla3* mutant knock-in (A) and wild-type mice (B). (C) Representative images of collagen immunohistochemistry in liver sections (black scale bar represents 100 μm). Liver hydroxyproline levels in *Pnpla3* mutant knock-in (D) and wild-type mice (E). Values are presented as the mean ± SEM. *P* values were calculated using 2-sided *t*-tests. Abbreviations: ASO: antisense oligonucleotide; Col1a1: collagen type I alpha 1 chain; Ctrl: control; Rplp0: ribosomal protein large P0. Mutant knock-in mice are defined as homozygotes for a methionine (M) at position 148 of the Pnpla3 protein, while wild-type littermates are homozygotes for an isoleucine (I) at the same position. WT: wild-type; MUT: mutant.

levels of PUFAs in lipid droplets after Pnpla3 ASO treatment irrespective of the genotype. This may be due to either a redistribution of PUFAs channeled into the triglycerides in the tissue, or directly related to the decrease in MUFAs. A previous study on the lipidome of purified hepatic lipid droplets suggests a potential novel enzymatic activity of Pnpla3 acquired specifically by the mutant protein [32]. Results of our analyses are in line with this hypothesis. A previous study on the liver lipidome of humans indicate that PNPLA3 148M mutant allele carriers have more polyunsaturated triacylglycerols than wild-type allele carriers [33]. However, in a recent study, when high liver fat to normal liver fat groups were compared, PNPLA3 wild-type and mutant allele carriers showed similar lipid changes although wild-type carriers presented with a higher proportion of specific diacylglycerols that may explain the dissociation between liver fat and insulin resistance in PNPLA3 148M mutant allele carriers [34]. Noteworthy, these human lipidomic studies were performed in whole liver specimens (as opposed to purified lipid droplets in this study) making results a bit difficult to compare.

We found lower circulating haptoglobin levels, liver macrophage content, and moderately reduced lobular inflammation after Pnpla3 ASO treatment in the *Pnpla3* mutant knock-in mice, but not in the wild-type mice. Haptoglobin is an acute phase protein produced by the liver and also by the adipose tissue [35] where we also observed a suppression of Pnpla3 after treatment. Therefore, we cannot rule out that plasma haptoglobin levels were influenced by reduced inflammation in the adipose tissue. However, plasma haptoglobin correlates to the degree of adiposity [36] and the Pnpla3 ASO treatment did not affect body weight or adiposity. Pnpla3 ASO treatment specifically reduced liver Mcp1 levels in the *Pnpla3* mutant knock-in mice, but not in the wild-type mice. Mcp1 and its receptor C–C chemochine receptor-2 (Ccr2) play a pivotal role in recruiting monocytes/macrophages to sites of inflammation in the liver [37,38]. In addition, haptoglobin can attract monocytes/macrophages in part through its interaction with Ccr2 [35]. Genetic deletion of Mcp1 or Ccr2 and Ccr2 inhibition protect from liver inflammation [37,39]. Thus, Pnpla3 silencing may decrease liver inflammation specifically through down-regulation of liver Mcp1 in *Pnpla3* mutant knock-in mice.

When we examined liver fibrosis, we found a consistent Pnpla3 ASO-mediated reduction in both the liver collagen expression and fibrosis severity in the *Pnpla3* mutant knock-in mice but not in the wild-type mice. We also found lower hepatic Timp2 protein levels present only in the mutant knock-in mice. TIMP2 expression levels are elevated in activated human hepatic stellate cells [40] and in fibrotic rat livers [41]. Moreover, TIMP2 directly inhibits the collagenolytic activity of MMP2

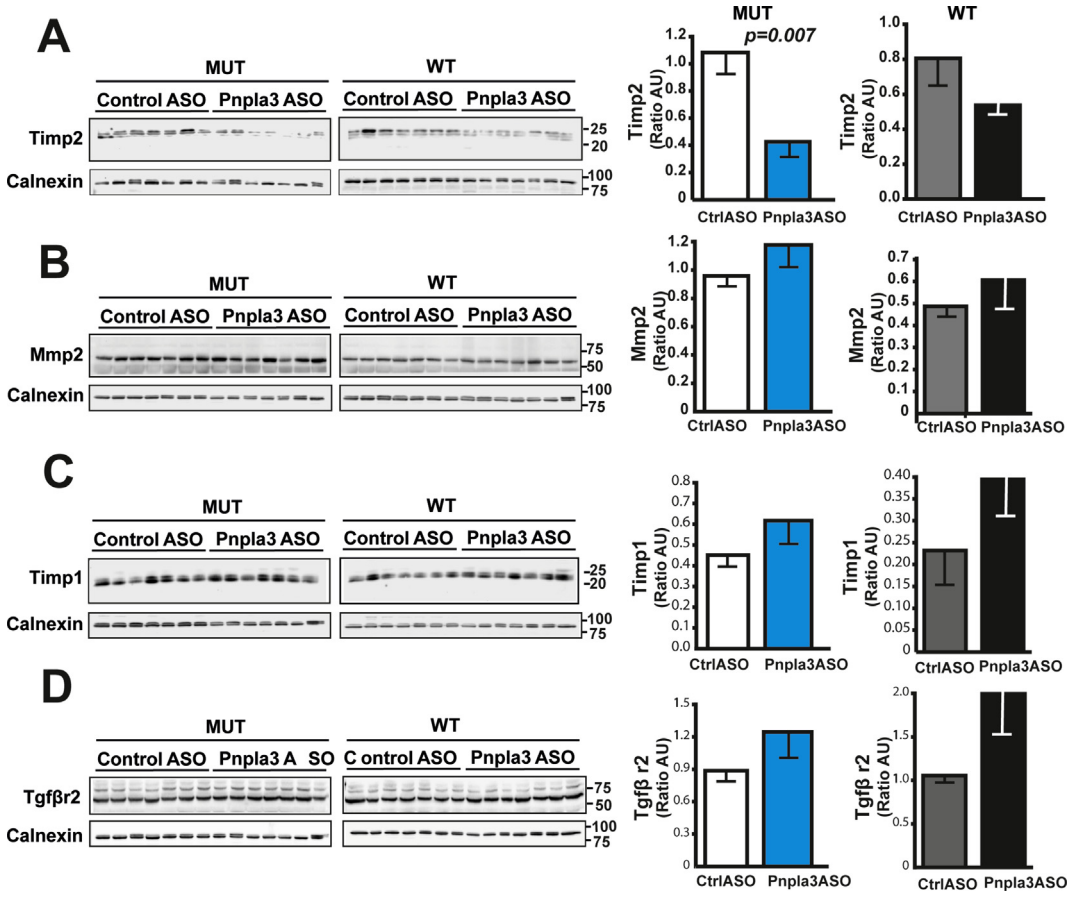

Figure 7: The Pnpla3 ASO treatment reduced liver Timp2 protein levels in *Pnpla3* mutant knock-in mice fed a NASH-inducing diet. Homozygous *Pnpla3* mutant knock-in and wild-type littermates were fed a NASH-inducing diet for 26 weeks. After 12 weeks of feeding on the NASH diet, *Pnpla3* mutant knock-in and wild-type mice were treated with either control or Pnpla3 ASOs (5 mg/kg/week administered by two subcutaneous injections per week, $n = 8–9$ mice/group) for 14 weeks. Liver protein levels of Timp2 (A), Mmp2 (B), Timp1 (C), and Tgfβr2 (D) measured with western blot analyses. Values are presented as the mean ± SEM. *P* values were calculated using 2-sided *t*-tests. Abbreviations: ASO: antisense oligonucleotide; Mmp2: matrix metalloproteinase 2; Tgfβr2: transforming growth factor, beta receptor 2; Timp: tissue inhibitor of metalloproteinase. Mutant knock-in mice are defined as homozygotes for a methionine (M) at position 148 of the Pnpla3 protein, while wild-type littermates are homozygotes for an isoleucine (I) at the same position. WT: wild-type; MUT: mutant.

[42] which is increased in experimental models of fibrosis and in humans with chronic liver disease [43–47]. Finally, we have shown *in vitro* and *ex vivo* that PNPLA3 has retinyl esters activity and the mutant, predisposing to more severe fibrosis, has higher secretion of TIMP2 [48]. Thus, the specific reduction in liver fibrosis in mutant mice seems to be dependent on a higher collagenolytic activity mediated by lower Timp2 secretion from hepatic stellate cells. Notably, Pnpla3 silencing in wild-type mice reduced the hepatic mRNA levels of the *Col1a1* and tended to reduce the liver collagen content and Timp2 expression levels. Based on these data, a study with a longer duration and more animals might reveal a beneficial effect of the Pnpla3 ASO treatment also in the wild-type mice.

Taken all this together, we show a specific effect in reducing liver inflammation and fibrosis after suppression of Pnpla3 specifically in the mutant knock-in mice. This effect could be due to: a) decreased inflammation caused by lower levels of chemokine attracting inflammatory cells, b) higher collagen breakdown resulting from the inhibition of a tissue metalloproteinase family member, and c) a direct beneficial effect of reducing the accumulation of the potentially toxic mutant protein on lipid droplets.

In terms of translation into human treatments, suppression of the synthesis of the PNPLA3 protein may be beneficial in patients presenting with NAFLD. Importantly, the suppression of this protein would ameliorate liver inflammation and fibrosis, the main variables underlying the clinical outcomes, more markedly in individuals who are homozygous for the PNPLA3 148M mutant protein. In addition, several improvements were also seen in wild-type mice indicating that such a therapy may also prove to be beneficial in wild type allele carriers. Currently, no approved drugs efficiently curing NAFLD or NASH are available. However, several treatment options are currently being evaluated in clinical trials [1,4,49]. Thus, a variety of pathway-specific drugs designed to treat NAFLD and NASH will probably emerge in the future. However, this preclinical study provides a proof of concept evidence for a precision medicine approach as a treatment for NASH by identifying a sub-population (*PNPLA3* 148M allele carriers) that may be high responders to a PNPLA3 ASO therapy. Thus, this therapeutic approach exploits a common innate genetic risk variant to ameliorate the disease using delivery of a $GalNAc_3$-conjugated PNPLA3 ASO to liver cells.

In conclusion, we show that *Pnpla3* silencing exerts a beneficial effect, more pronounced in the presence of the Pnpla3 148M mutation, on liver fat accumulation, inflammation, and fibrosis. Further studies are needed to assess whether these findings will translate to humans.

DISCLOSURES

S.R. has been consulting for AstraZeneca, GSK, Celgene Corporation and Pfizer in the last 5 years and he received Research Grant from AstraZeneca. D.L., A.A., I.A., A-C.A., K.M-B., M.Z., A.L., M.B., G.B., M.B-Y., W.G.H., B.C., and P.Å. are AstraZeneca employees. M.G., R.L., S.M., and S.B. are Ionis Pharmaceuticals employees. All other authors have none to declare.

FINANCIAL SUPPORT

This work was supported by the Swedish Research Council [Vetenskapsrådet (VR), 2016-01527], the Swedish Heart-Lung Foundation [20120533], the Swedish federal government funding under the Agreement on Medical Training and Medical Research (ALF) [716731], the Novonordisk Foundation Grant for Excellence in Endocrinology [Excellence Project, 9321-430], the Swedish Diabetes Foundation [DIA 2017-205], a research grant from AstraZeneca [Echo Project, 10033852], Wallenberg Academy Fellows from the Knut and Alice Wallenberg Foundation [KAW 2017.0203] (SR), and the Wilhelm and Martina Lundgren Science Fund [2016-1255] (RMM). AIRC [MFAG N. 16888] and Italian Ministry of Health [RF-2016-02364358] (LV).

ACKNOWLEDGMENTS

We thank Prof. Helen Hobbs at the University of Texas Southwestern Medical Center at Dallas, TX, USA, for kindly providing the antibody against Pnpla3 used in the present study. We thank Therese Hagstedt and Daniel Karlsson at CVRM, IMED Biotech Unit, AstraZeneca, Gothenburg, Sweden, for providing excellent technical assistance and Laboratory Animal Sciences, AstraZeneca, Gothenburg, Sweden, for assisting with these studies.

CONFLICT OF INTEREST

None declared.

APPENDIX A. SUPPLEMENTARY DATA

Supplementary data to this article can be found online at https://doi.org/10.1016/j.molmet.2019.01.013.

REFERENCES

[1] Younossi, Z.M., Koenig, A.B., Abdelatif, D., Fazel, Y., Henry, L., Wymer, M., 2016. Global epidemiology of nonalcoholic fatty liver disease-Meta-analytic assessment of prevalence, incidence, and outcomes. Hepatology 64(1): 73–84.

[2] Serfaty, L., Lemoine, M., 2008. Definition and natural history of metabolic steatosis: clinical aspects of NAFLD, NASH and cirrhosis. Diabetes and Metabolism 34(6 Pt 2):634–637.

[3] Dulai, P.S., Singh, S., Patel, J., Soni, M., Prokop, L.J., Younossi, Z., et al., 2017. Increased risk of mortality by fibrosis stage in nonalcoholic fatty liver disease: systematic review and meta-analysis. Hepatology 65(5): 1557–1565.

[4] Younossi, Z.M., Loomba, R., Rinella, M.E., Bugianesi, E., Marchesini, G., Neuschwander-Tetri, B.A., et al., 2018. Current and future therapeutic regimens for non-alcoholic fatty liver disease (NAFLD) and non-alcoholic steatohepatitis (NASH). Hepatology 68(1):349–360.

[5] Dongiovanni, P., Stender, S., Pietrelli, A., Mancina, R.M., Cespiati, A., Petta, S., et al., 2018. Causal relationship of hepatic fat with liver damage and insulin resistance in nonalcoholic fatty liver. Journal of Internal Medicine 283(4):356–370.

[6] Eslam, M., Valenti, L., Romeo, S., 2018. Genetics and epigenetics of NAFLD and NASH: clinical impact. Journal of Hepatology 68(2):268–279.

[7] Romeo, S., Kozlitina, J., Xing, C., Pertsemlidis, A., Cox, D., Pennacchio, L.A., et al., 2008. Genetic variation in PNPLA3 confers susceptibility to nonalcoholic fatty liver disease. Nature Genetics 40(12):1461–1465.

[8] Trépo, E., Romeo, S., Zucman-Rossi, J., Nahon, P., 2016. PNPLA3 gene in liver diseases. Journal of Hepatology 65(2):399–412.

[9] Stender, S., Kozlitina, J., Nordestgaard, B.G., Tybjærg-Hansen, A., Hobbs, H.H., Cohen, J.C., 2017. Adiposity amplifies the genetic risk of fatty liver disease conferred by multiple loci. Nature Genetics 49(6):842–847.

[10] Romeo, S., Sentinelli, F., Dash, S., Yeo, G.S., Savage, D.B., Leonetti, F., et al., 2010. Morbid obesity exposes the association between PNPLA3 I148M (rs738409) and indices of hepatic injury in individuals of European descent. International Journal of Obesity (London) 34(1):190–194.

[11] Romeo, S., Sentinelli, F., Cambuli, V.M., Incani, M., Congiu, T., Matta, V., et al., 2010. The 148M allele of the PNPLA3 gene is associated with indices of liver damage early in life. Journal of Hepatology 53(2):335–338.

[12] He, S., McPhaul, C., Li, J.Z., Garuti, R., Kinch, L., Grishin, N.V., et al., 2010. A sequence variation (I148M) in PNPLA3 associated with nonalcoholic fatty liver disease disrupts triglyceride hydrolysis. Journal of Biological Chemistry 285(9):6706–6715.

[13] Pingitore, P., Pirazzi, C., Mancina, R.M., Motta, B.M., Indiveri, C., Pujia, A., et al., 2014. Recombinant PNPLA3 protein shows triglyceride hydrolase activity and its I148M mutation results in loss of function. Biochimica et Biophysica Acta 1841(4):574–580.

[14] Pirazzi, C., Valenti, L., Motta, B.M., Pingitore, P., Hedfalk, K., Mancina, R.M., et al., 2014. PNPLA3 has retinyl-palmitate lipase activity in human hepatic stellate cells. Human Molecular Genetics 23(15):4077–4085.

[15] BasuRay, S., Smagris, E., Cohen, J.C., Hobbs, H.H., 2017. The PNPLA3 variant associated with fatty liver disease (I148M) accumulates on lipid droplets by evading ubiquitylation. Hepatology 66(4):1111–1124.

[16] Pirazzi, C., Adiels, M., Burza, M.A., Mancina, R.M., Levin, M., Ståhlman, M., et al., 2012. Patatin-like phospholipase domain-containing 3 (PNPLA3) I148M (rs738409) affects hepatic VLDL secretion in humans and in vitro. Journal of Hepatology 57(6):1276–1282.

[17] Pingitore, P., Dongiovanni, P., Motta, B.M., Meroni, M., Lepore, S.M., Mancina, R.M., et al., 2016. PNPLA3 overexpression results in reduction of proteins predisposing to fibrosis. Human Molecular Genetics 25(23): 5212–5222.

[18] Smagris, E., BasuRay, S., Li, J., Huang, Y., Lai, K.M., Gromada, J., et al., 2015. Pnpla3I148M knockin mice accumulate PNPLA3 on lipid droplets and develop hepatic steatosis. Hepatology 61(1):108–118.

[19] Li, J.Z., Huang, Y., Karaman, R., Ivanova, P.T., Brown, H.A., Roddy, T., et al., 2012. Chronic overexpression of PNPLA3I148M in mouse liver causes hepatic steatosis. Journal of Clinical Investigation 122(11):4130–4144.

[20] Chen, W., Chang, B., Li, L., Chan, L., 2010. Patatin-like phospholipase domain-containing 3/adiponutrin deficiency in mice is not associated with fatty liver disease. Hepatology 52(3):1134–1142.

[21] Basantani, M.K., Sitnick, M.T., Cai, L., Brenner, D.S., Gardner, N.P., Li, J.Z., et al., 2011. Pnpla3/Adiponutrin deficiency in mice does not contribute to fatty liver disease or metabolic syndrome. The Journal of Lipid Research 52(2):318–329.

[22] Palmer, C.N., Maglio, C., Pirazzi, C., Burza, M.A., Adiels, M., Burch, L., et al., 2012. Paradoxical lower serum triglyceride levels and higher type 2 diabetes mellitus susceptibility in obese individuals with the PNPLA3 148M variant. PLoS One 7(6):e39362.

[23] Donati, B., Motta, B.M., Pingitore, P., Meroni, M., Pietrelli, A., Alisi, A., et al., 2016. The rs2294918 E434K variant modulates patatin-like phospholipase domain-containing 3 expression and liver damage. Hepatology 63(3):787–798.

[24] Abul-Husn, N.S., Cheng, X., Li, A.H., Xin, Y., Schurmann, C., Stevis, P., et al., 2018. A protein-truncating HSD17B13 variant and protection from chronic liver disease. New England Journal of Medicine 378(12):1096–1106.

[25] Kumashiro, N., Yoshimura, T., Cantley, J.L., Majumdar, S.K., Guebre-Egziabher, F., Kursawe, R., et al., 2013. Role of patatin-like phospholipase domain-containing 3 on lipid-induced hepatic steatosis and insulin resistance in rats. Hepatology 57(5):1763–1772.

[26] Kumari, M., Schoiswohl, G., Chitraju, C., Paar, M., Cornaciu, I., Rangrez, A.Y., et al., 2012. Adiponutrin functions as a nutritionally regulated lysophosphatidic acid acyltransferase. Cell Metabolism 15(5):691–702.

[27] Schmidt, K., Prakash, T.P., Donner, A.J., Kinberger, G.A., Gaus, H.J., Low, A., et al., 2017. Characterizing the effect of GalNAc and phosphorothioate backbone on binding of antisense oligonucleotides to the asialoglycoprotein receptor. Nucleic Acids Research 45(5):2294–2306.

[28] Clapper, J.R., Hendricks, M.D., Gu, G., Wittmer, C., Dolman, C.S., Herich, J., et al., 2013. Diet-induced mouse model of fatty liver disease and nonalcoholic steatohepatitis reflecting clinical disease progression and methods of assessment. American Journal of Physiology - Gastrointestinal and Liver Physiology 305(7):G483–G495.

[29] Trevaskis, J.L., Griffin, P.S., Wittmer, C., Neuschwander-Tetri, B.A., Brunt, E.M., Dolman, C.S., et al., 2012. Glucagon-like peptide-1 receptor agonism improves metabolic, biochemical, and histopathological indices of nonalcoholic steatohepatitis in mice. American Journal of Physiology - Gastrointestinal and Liver Physiology 302(8):G762–G772.

[30] Tølbøl, K.S., Kristiansen, M.N., Hansen, H.H., Veidal, S.S., Rigbolt, K.T., Gillum, M.P., et al., 2018. Metabolic and hepatic effects of liraglutide, obeticholic acid and elafibranor in diet-induced obese mouse models of biopsy-confirmed nonalcoholic steatohepatitis. World Journal of Gastroenterology 24(2):179–194.

[31] Kleiner, D.E., Brunt, E.M., Van Natta, M., Behling, C., Contos, M.J., Cummings, O.W., et al., 2005. Design and validation of a histological scoring system for nonalcoholic fatty liver disease. Hepatology 41(6):1313–1321.

[32] Mitsche, M.A., Hobbs, H.H., Cohen, J.C., 2018. Phospholipase domain-containing protein 3 promotes transfers of essential fatty acids from triglycerides to phospholipids in hepatic lipid droplets. Journal of Biological Chemistry 293(18):6958–6968.

[33] Luukkonen, P.K.Z.Y., Sädevirta, S., Leivonen, M., Arola, J., Orešič, M., Hyötyläinen, T., et al., 2016. Hepatic ceramides dissociate steatosis and insulin resistance in patients with non-alcoholic fatty liver disease. Journal of Hepatology 64(5):1167–1175.

[34] Franko, A., Merkel, D., Kovarova, M., Hoene, M., Jaghutriz, B., Heni, M., et al., 2018. Dissociation of fatty liver and insulin resistance in I148M PNPLA3 carriers: differences in diacylglycerol (DAG) FA18:1 lipid species as a possible explanation. Nutrients 10(9):1314.

[35] Maffei, M., Barone, I., Scabia, G., Santini, F., 2016. The multifaceted haptoglobin in the context of adipose tissue and metabolism. Endocrine Reviews 37(4):403–416.

[36] Chiellini, C., Bertacca, A., Novelli, S.E., Gorgun, C.Z., Ciccarone, A., Giordano, A., et al., 2002. Obesity modulates the expression of haptoglobin in the white adipose tissue via TNFalpha. Journal of Cellular Physiology 190(2):251–258.

[37] Kanda, H., Tateya, S., Tamori, Y., Kotani, K., Hiasa, K.I., Kitazawa, R., et al., 2006. MCP-1 contributes to macrophage infiltration into adipose tissue, insulin resistance, and hepatic steatosis in obesity. Journal of Clinical Investigation 116(6):1494–1505.

[38] Obstfeld, A.E., Sugaru, E., Thearle, M., Francisco, A.M., Gayet, C., Ginsberg, H.N., et al., 2010. C-C chemokine receptor 2 (CCR2) regulates the hepatic recruitment of myeloid cells that promote obesity-induced hepatic steatosis. Diabetes 59(4):916–925.

[39] Tamura, Y., Sugimoto, M., Murayama, T., Ueda, Y., Kanamori, H., Ono, K., et al., 2008. Inhibition of CCR2 ameliorates insulin resistance and hepatic steatosis in db/db mice. Arteriosclerosis, Thrombosis, and Vascular Biology 28(12):2195–2201.

[40] Xu, L., Hui, A.Y., Albanis, E., Arthur, M.J., O'Byrne, S.M., Blaner, W.S., et al., 2005. Human hepatic stellate cell lines, LX-1 and LX-2: new tools for analysis of hepatic fibrosis. Gut 54(1):142–151.

[41] Peng, J., Li, X., Feng, Q., Chen, L., Xu, L., Hu, Y., 2013. Anti-fibrotic effect of Cordyceps sinensis polysaccharide: inhibiting HSC activation, TGF-beta1/Smad signalling, MMPs and TIMPs. Experimental Biology and Medicine (Maywood) 238(6):668–677.

[42] Stetler-Stevenson, W.G., Krutzsch, H.C., Liotta, L.A., 1989. Tissue inhibitor of metalloproteinase (TIMP-2). A new member of the metalloproteinase inhibitor family. Journal of Biological Chemistry 264(29):17374–17378.

[43] Milani, S., Herbst, H., Schuppan, D., Grappone, C., Pellegrini, G., Pinzani, M., et al., 1994. Differential expression of matrix-metalloproteinase-1 and -2 genes in normal and fibrotic human liver. American Journal Of Pathology 144(3):528–537.

[44] Takahara, T., Furui, K., Funaki, J., Nakayama, Y., Itoh, H., Miyabayashi, C., et al., 1995. Increased expression of matrix metalloproteinase-II in experimental liver fibrosis in rats. Hepatology 21(3):787–795.

[45] Benyon, R.C., Iredale, J.P., Goddard, S., Winwood, P.J., Arthur, M.J.P., 1996. Expression of tissue inhibitor of metalloproteinases 1 and 2 is increased in fibrotic human liver. Gastroenterology 110(3):821–831.

[46] Takahara, T., Furui, K., Yata, Y., Jin, B., Zhang, L.P., Nambu, S., et al., 1997. Dual expression of matrix metalloproteinase-2 and membrane-type 1-matrix metalloproteinase in fibrotic human livers. Hepatology 26(6):1521–1529.

[47] Preaux, A.M., Mallat, A., Nhieu, J.T., D'Ortho, M.P., Hembry, R.M., Mavier, P., 1999. Matrix metalloproteinase-2 activation in human hepatic fibrosis regulation by cell-matrix interactions. Hepatology 30(4):944–950.

[48] Pirazzi, C., Valenti, L., Motta, B.M., Pingitore, P., Hedfalk, K., Mancina, R.M., et al., 2014. PNPLA3 has retinyl-palmitate lipase activity in human hepatic stellate cells. Human Molecular Genetics 23(15):4077–4085.

[49] Rinella, M.E., Sanyal, A.J., 2016. Management of NAFLD: a stage-based approach. Nature Reviews Gastroenterology & Hepatology 13(4):196–205.

